Potential Surface Improvements by Bump Removal for 64-m Antenna

S. Katow and C. N. Guiar
Ground Antenna and Facilities Engineering Section

The surface panels of the main reflector of the 64-m antenna are initially set at an elevation angle of 45 deg, where most tracking occurs, to ideally match a prescribed paraboloid. As the antenna is rotated about the elevation axis, distortions are introduced at the surface panel's supporting nodes as well as at the main reflector backup structure by changes in the direction of the gravity forces relative to the reflector symmetric axis. Major bump displacements could be corrected by controlling the position of the surface-panel corners using adjustable mechanical jacks that change in length with the antenna elevation angle. The analysis of two bump-removal configurations is presented and one unique adjustment mechanism is proposed. A gain recovery of 0.2 dB at X-band would be available if the reflector structure distortion rms were reduced from 0.63 mm (0.025 in.) to 0.15 mm (0.006 in.).

I. Introduction

Antenna surface-panel distortions and deflections caused by changes in gravity loading are introduced by antenna rotation about the elevation axis. These gravity-induced deflections result in differences in the radio-frequency (RF) path-lengths, thus contributing to the RF gain losses of the antenna. The gain loss is a function of, among other parameters, the root-mean-square (rms) of the distortions of the main reflector and of the operating frequency being used.

As the planetary exploration program continues to grow, the need for an efficient antenna system that provides increased gain, performance, and productivity becomes evident. Upgrading the present 64-m antenna network to improve performance and gain proves to be economically more practical than building a new replacement system. Viable modifications, presently under investigation, include extending the reflector aperture to 70-m, improving the surface panel fabrication accuracy and setting precision, reducing the gravity-induced distortions by stiffening braces, and increasing the operating frequency (Ref. 1).

This article describes one additional possible modification in upgrading the 64-m antenna. It calls for the correction of major displacements by controlling, on a real-time basis, the height of the surface panel's corners using mechanical means, with corrections changing with the elevation angle changes.

A preliminary study of the potential benefits (Ref. 2) resulted in an improved surface with less distortions (rms value), where simplified assumptions of displacement in the major bumpy areas were made. This report, a follow-up to the prior study, describes an improved computational technique used to determine the nodal corrections necessary to reduce the surface tolerance. A conceptual mechanical design to implement the corrections is also presented in this report.

II. Analysis

Since the surface panels of the 64-m antenna are initially set at an elevation angle of 45 deg to match a prescribed paraboloid, gravity-induced distortions are introduced at the horizon, zenith attitude, or any position in between while the antenna rotates about the elevation axis.

The distortion vectors of the joints (or nodes) in the structure supporting the reflector panels are first computed for unit gravity loading (one g where g is the acceleration of gravity) in each of the symmetric and antisymmetric directions as shown in Fig. 1. Either NASTRAN or IDEAS (in-house) structural analysis computer programs can be used for this purpose. Using the relationship of the unit gravity load vectors and their components in the symmetric and antisymmetric directions, as shown in Fig. 1, the three-dimensional distortion vectors at any elevation angle are given by:

$$\mathbf{d}_\theta = (\sin\theta - \sin\theta_s)\,\mathbf{U}_{sym} + (\cos\theta - \cos\theta_s)\,\mathbf{U}_{antisym} \quad (1)$$

where

$\mathbf{U}_{sym}$ = symmetric, unit gravity distortion vector for gravity off to on at θ_s

$\mathbf{U}_{antisym}$ = unit gravity distortion vector for gravity off to on at θ_s

$\mathbf{d}_\theta$ = gravity distortion vector at angle θ

θ = antenna elevation angle

θ_s = elevation angle at which panels are set (usually 45 deg)

The RMS program (Ref. 3) is used to compute the "normal" surface errors (perpendicular to reflector surface) at a specific elevation angle (θ) using the two sets of deflections $\mathbf{d}_{sym}$ and $\mathbf{d}_{antisym}$. Only two sets of deflection data (for the first and fourth quadrants of the antenna) are supplied to the RMS program. Data for the second and third quadrants are generated by symmetry. The RMS program multiplies both sets of deflection data by the appropriate angular functions in Eq. (1), adds the resulting weighted deflections, and computes the surface normal errors after making a paraboloid best fit that minimizes the pathlength errors. For the antenna horizon-look case ($\theta = 0°$) at $\theta_s = 45$ deg, the distortion vector ($\mathbf{d}_0$) is formed as:

$$\mathbf{d}_0 = -0.707\,\mathbf{U}_{sym} + 0.293\,\mathbf{U}_{antisym} \quad (2)$$

and for the zenith-look case ($\theta = 90$ deg) at $\theta_s = 45$ deg,

$$\mathbf{d}_{90} = 0.293\,\mathbf{U}_{sym} - 0.707\,\mathbf{U}_{antisym} \quad (3)$$

The output of the rms program provides two types of normal errors: (1) no-fit error and (b) best-fit error. One file outputs the no-fit normal errors and another file outputs the best-fit normal errors. The no-fit normal error is the total distortion vector due to gravity loading changes as the antenna rotates from the setting elevation angle (θ_s) to the horizon or zenith configuration. This means that the no-fit normal errors are the three-component distortion vectors normalized to the given paraboloid surface.

The RMS program also outputs the best-fit root-mean-square value of the ½-pathlength error data together with a contour map of the normal errors. Contour maps of the gravity off/on distortions for the 64-m antenna measured normal to the surface of the best-fit paraboloid for the antisymmetric horizon-look ($\theta = 0$ deg) and symmetric zenith-look ($\theta = 90$ deg) cases are shown in Figs. 2 and 3, respectively.

The surface distortion contour maps for the unit gravity (off to on) loading vector provide important information. Inspection of the contour maps in Figs. 2 and 3 for the **U** vectors show major displacements, hereafter referred to as "bumps." Removing these bumps would minimize the overall distortion (rms) of the main reflector, thus increasing the gain of the antenna. Since the bumps, from Figs. 2 and 3, are on distinctly different parts of the paraboloid surface, i.e., independent, it can be assumed that bump nodes for the zenith-look case ($\theta = 90$ deg) are affected only by symmetric gravity loading, and bump nodes for the horizon-look case ($\theta = 0$ deg) are affected only by antisymmetric gravity loading. This independence of bumps at these two extreme positions allows the use of eccentric rollers (driven by the rotation of the elevation-axis shaft) to reduce gravity distortions. The eccentric rollers produce sine and cosine linear functions of the elevation angle, θ, that match, by proper design, the desired distortion compensation due to gravity loading changes.

Note that the distortion (in rms) for the unit symmetric loading is 0.863 mm, which is larger than the 0.616 mm for the unit antisymmetric loading vector. Therefore, the horizon-look case was selected in this study for corrections at selected

nodes since 0.7 part of the symmetric loading change occurs from 45-deg elevation to horizon-look. Another reason for that selection was the fact that the DSN 64-m antenna is used most frequently between the 45-deg to horizontal position range. The analytical technique used to determine the most effective node corrections is described in the following section.

III. Trial Computations

The analysis for determining the bump corrections for the 64-m antenna was done in two parts. The first part determined the necessary bump-node corrections for the horizon-look case. The second part of the correction analysis determined the relationship between the horizon-look and zenith-look corrections, which generated the necessary bump-node corrections and the new overall rms where the zenith-look gravity distortions were initially assumed to be due to the symmetric gravity loading vector only. Therefore, the initial zenith-look surface corrections are a function of the correction made at horizon-look.

The RMS program, using the three-component distortion data from the structural programs, produced at each node a listing of both the no-fit normal errors and the best-fit normal errors (after best fitting of the paraboloid). By examining the best-fit contour map of the horizon-look case, with the surface panels set at 45-deg elevation, a number of large, bump-displacement nodes were observed. Data for 157 nodes were entered in the program with zero displacements as a baseline from which corrections could start.

An initial set of corrected nodes was generated after subtracting the best-fit normal errors from the no-fit normal errors for the large displacement nodes. This correction corresponds to the distance from the actual paraboloid to the best-fit paraboloid and results in a substantially improved rms of 0.27 mm (0.0107 in.). The best-fit results associated with this new rms represent the normal errors to the corrections provided by the new deflection data.

Additional corrections to the selected set of bump nodes were attempted to improve further the overall rms. In the first node-correction attempt, (option-1 design) the best-fit normal errors were subtracted directly from the no-fit normal errors. Subtraction was necessary to determine the distance between the actual paraboloid and the best-fit paraboloid. Since the new best-fit data produced a best-fit paraboloid for which the vertex is shifted in the Z direction as the bump-node errors are removed, the new best-fit paraboloid must be shifted so that its vertex coincides with that of the no-fit paraboloid. An over-correction factor of 1.8 was used to compensate for this offset. A new set of corrected nodes can therefore be generated by subtracting the new best-fit data, multiplied by the over-correction factor, from the first set of corrected node data. This new set of corrected nodes resulted in an improved overall rms of 0.18 mm (0.007 in.).

Some surface nodes originally gave a best-fit rms near zero, thus misleadingly eliminating the need for any further corrections. However, repeated corrections of other nodes shifted the best-fit paraboloid in the Z direction by approximately 0.50 mm (0.020 in.), giving the originally "good" nodes a poor rms. To fine-tune the corrections made thus far, 63 of these nodes were given a correction designed to compensate for the shift in the Z direction. The final rms for (157 + 63) or 210 corrected nodes (with the surface panels set at 45 deg) is 0.15 mm (0.006 in.). The structural model for the selected nodes of this case is shown in Fig. 4. Figures 5 and 6 show the contour maps of the distortions measured normal to the surface of the best-fit paraboloid before and after the bumps are removed for the horizon-look case.

Corrections for the zenith-look case are made for the same nodes as for the horizon-look case and are initially assumed to be affected by symmetric gravity loading only. Therefore the zenith-look case (θ_Z) corrections are functions of the horizon-look (θ_H) case corrections and are given as:

$$\begin{aligned}\text{sym-gravity corrections} &= (\text{hor-look corrections})\,\frac{(\sin\theta_Z - \sin\theta_s)}{(\sin\theta_H - \sin\theta_s)} \\ &= (\text{hor-look corrections})\,\frac{0.3}{0.7} \end{aligned} \tag{4}$$

and for antisymmetric distortions:

$$\text{antisym-gravity corrections} = (\text{hor-look corrections})\,\frac{(\cos\theta_Z - \cos\theta_s)}{(\cos\theta_H - \cos\theta_s)} \tag{5}$$

where θ_Z is 90 deg, θ_H is 0 deg, and θ_s = 45 deg.

The initial set of corrected nodes for the zenith-look case was generated using Eqs. (4) and (5) after determining the rms using the initial set of corrected nodes. It was found that the prior assumption that the zenith-look case has only symmetric gravity loading is not quite accurate. Most of the nodes, however, agree with that assumption, but a few have distortions due to both symmetric and antisymmetric gravity loadings. The multiplication factors for the nodes exhibiting these traits were scaled accordingly and produced a final rms for the 220 corrected nodes (with the surface panels set at 45-deg elevation) of 0.23 mm (0.009 inches).

P. Potter (Ref. 1) designated a minimum acceptable surface tolerance for the 64-m antenna that allows efficient operation

at the 32-Ghz (Ka-band) frequency. The overall surface rms determined in this study for the zenith-look and horizon-look cases are below these tolerances. Reducing the number of nodes selected for this study will increase the overall rms to meet the minimum requirements of Ref. 1 and would result in a cost effective modification. The reduction effort, represented as option-2 design, results in an overall rms of 0.23 mm (0.009 in.) for the horizon-look case and 0.38 mm (0.015 in.) for the zenith-look case.

IV. Proposed Panel Adjustment Mechanism

The surface panels are supported from the reflector structure as shown in Fig. 7 by the inverted U-pads, which are now weld-connected to the top chords of the ribs. Figure 8 illustrates the proposed changes in the mounting of the inverted U-pads using flextures. The inverted U-pads can be pivoted to vary their heights up to the top chords of the reflector's rib trusses.

The proposed mechanism for raising or lowering the U-pad is illustrated in Fig. 9, and the mechanism is bolted to the U-pad and the top chord. An eccentrically mounted roller, which rotates in unison with the elevation axis, can provide the sine (θ) function as well as the amplitude change of the surface-panel position.

The driving flexible cables, connecting the antenna elevation shaft motion and the eccentric roller motion, can be driven in unison by a specially designed gearbox that has a large spur gear driving multiple smaller pinion gears placed around the periphery of the main gear. If there is excess torque capacity in the elevation drive, this special gearbox can be mounted on the alidade next to the elevation shaft protruding from the elevation bearing housing; the spur gear would be driven directly by the rotating elevation axis. The gearbox may also be driven by its own power unit using a simple switching device to maintain synchronous rotation with the elevation axis.

The angle of twist in the flexible driving cables between the special gearbox and the eccentric roller will determine the accuracy of the corrections imposed on the surface panels. The final design may require the use of a worm-gear reduction instead of the spur gear shown in Fig. 9. Initial cost estimates, however, show that further development is still needed.

V. Summary

This article has considered only the distortions of the main reflector surface resulting from gravity loading. Additional distortions result from both wind and temperature-difference loadings on the reflector structure, the surface panels, and the subreflector; these loadings become dominant for antenna operation at higher than X-band frequencies. Reflector nodes having major bump displacements could be corrected by controlling the position of the surface panel corners using adjustable mechanical jacks, which change position with changes in the antenna elevation angle. The analysis of two bump-removal configurations is presented in Table 1. The potential gain improvement is about 0.2 dB at X band (8.4 GHz) as the reflector surface distortion is reduced from 0.63 mm (0.025 in.) to 0.15 mm (0.006 in.). Although the proposed panel-adjustment mechanism can neutralize the nodal displacements at the selected corrected nodes, it requires future development effort and cost trade-off studies among other antenna upgrade options presently being implemented.

References

1. Potter, P. D., "64-Meter Antenna Operation at Ka-Band," in the *Deep Space Network Progress Report 42-57*, March and April 1980. Jet Propulsion Laboratory, Pasadena, Calif., pp. 65-70.

2. Katow, M. S., "A Proposed Method of Reducing the Gravity Distortions of the 64-Meter Antenna Main Reflector," in the *Deep Space Network Progress Report 42-23*, Oct. 1974. Jet Propulsion Laboratory, Pasadena, Calif., pp. 92-97.

3. Katow, M. S., and Schmele, L. W., "Antenna Structures: Evaluation Techniques of Reflector Distortions," in *Supporting Research and Advanced Development, Space Programs Summary 37-40*, Vol. IV, Sept. 30, 1968. Jet Propulsion Laboratory, Pasadena, California, pp. 73-76.

Table 1. Surface distortion (rms) due to gravity off/on loading

	Horizon position, mm (in.)	Zenith position, mm (in.)
Original 64-m antenna (structural only)	0.63 (0.025)	0.50 (0.020)
Upgrade option – 1 (220 corrected nodes)	0.15 (0.006)	0.23 (0.009)
Upgrade option – 2 (116 corrected nodes)	0.23 (0.009)	0.38 (0.015)

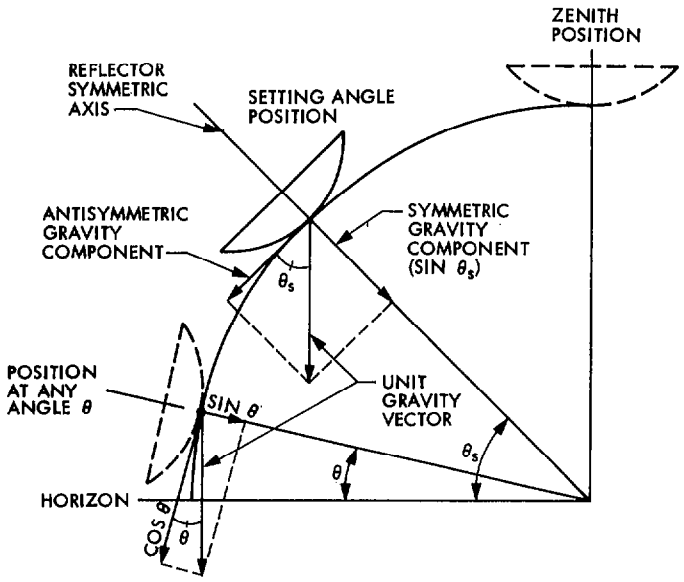

Fig. 1. Components of the gravity force vector

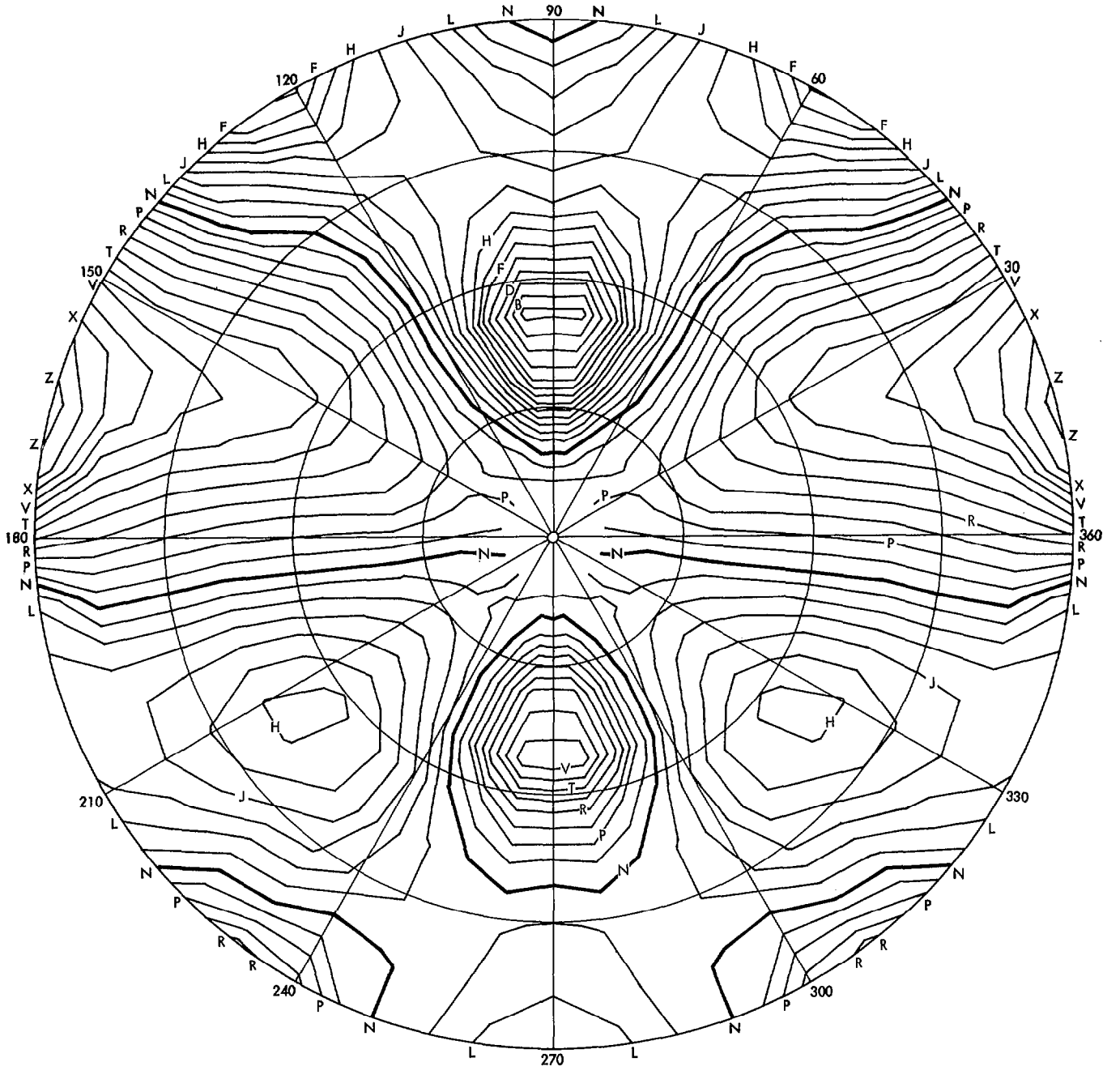

CONTOUR DEFINITIONS

NORMAL ERROR, mm	LABEL	NORMAL ERROR, mm	LABEL	NORMAL ERROR, mm	LABEL
-1.95	A	-0.60	J	0.75	S
-1.80	B	-0.45	K	0.90	T
-1.65	C	-0.30	L	1.05	U
-1.50	D	-0.15	M	1.20	V
-1.35	E	0.00	N	1.35	W
-1.20	F	0.15	O	1.50	X
-1.05	G	0.30	P	1.65	Y
-0.90	H	0.45	Q	1.80	Z
-0.75	I	0.60	R		

Fig. 2. Horizon-look (unit gravity, antisymmetric loading off/on) normal errors to best-fit paraboloid for existing 64-m antenna

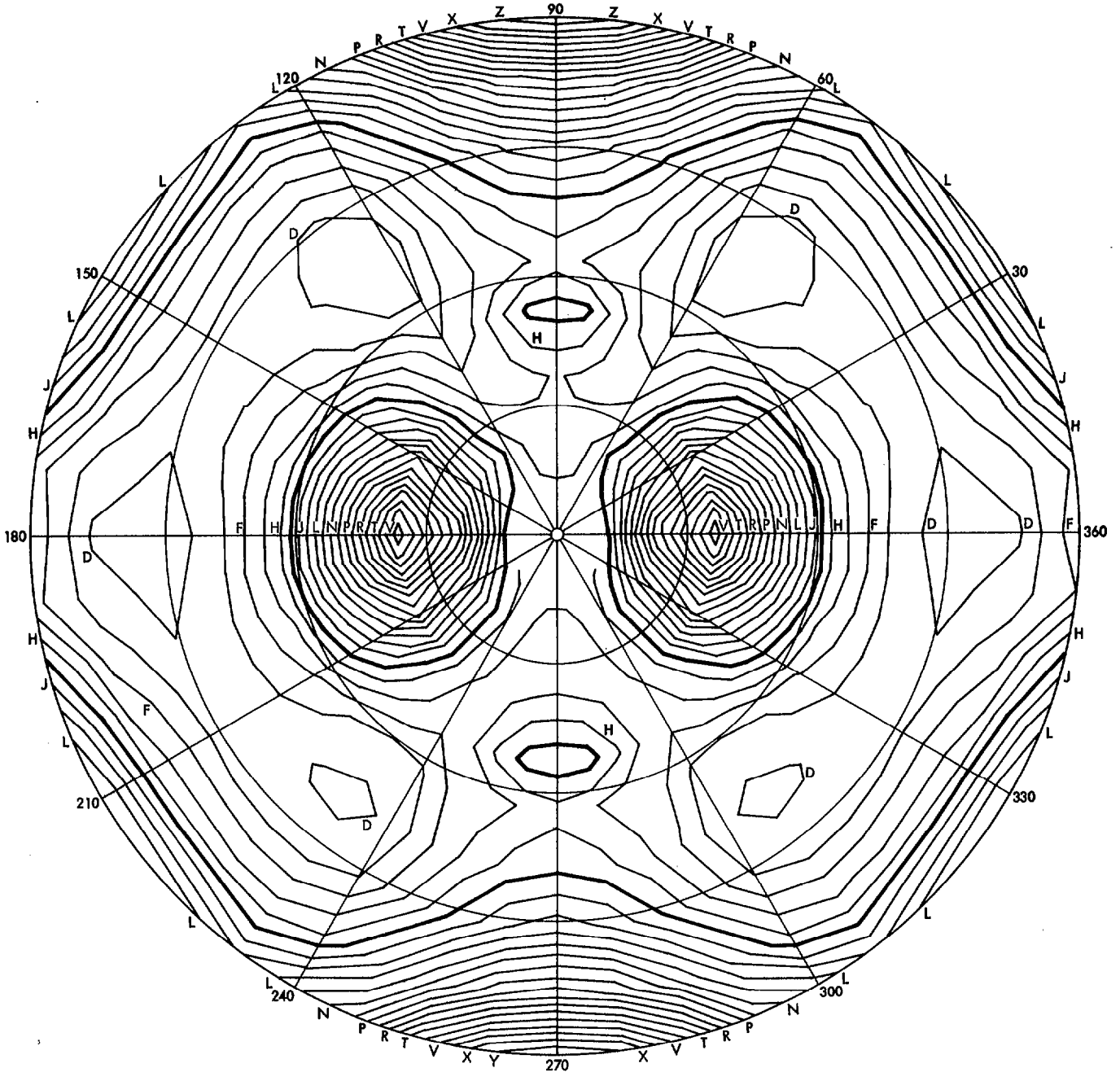

CONTOUR DEFINITIONS

NORMAL ERROR, mm	LABEL	NORMAL ERROR, mm	LABEL	NORMAL ERROR, mm	LABEL
-1.60	A	0.20	J	2.00	S
-1.40	B	0.40	K	2.20	T
-1.20	C	0.60	L	2.40	U
-1.00	D	0.80	M	2.60	V
-0.80	E	1.00	N	2.80	W
-0.60	F	1.20	O	3.00	X
-0.40	G	1.40	P	3.20	Y
-0.20	H	1.60	Q	3.40	Z
0.00	I	1.80	R		

Fig. 3. Zenith-look (unit gravity, symmetric loading off/on) normal errors to best-fit paraboloid for existing 64-m antenna

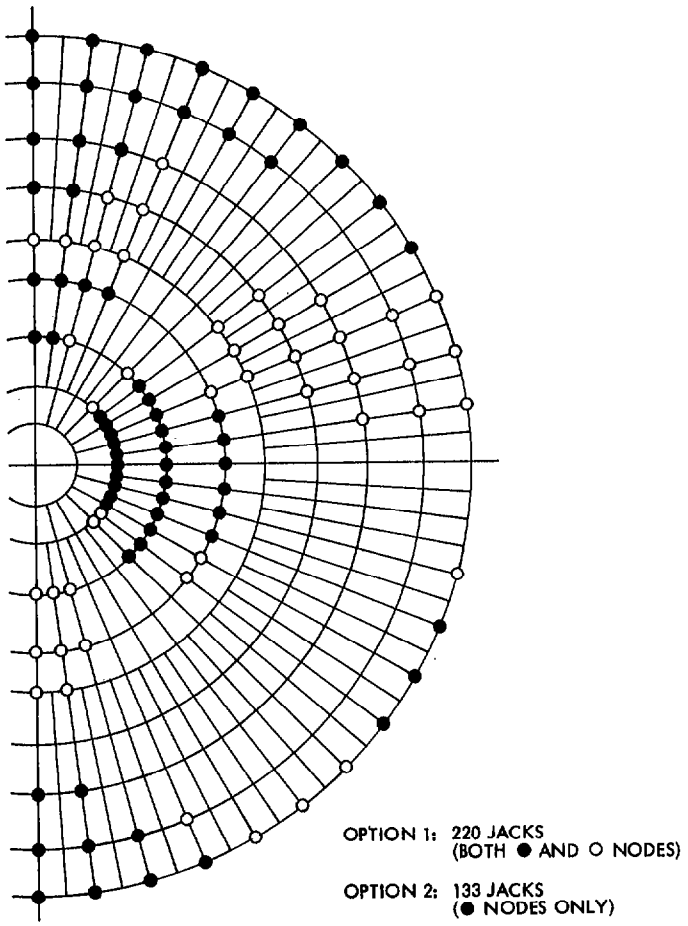

Fig. 4. Bump-removing adjustable jack stations for 64-m antenna

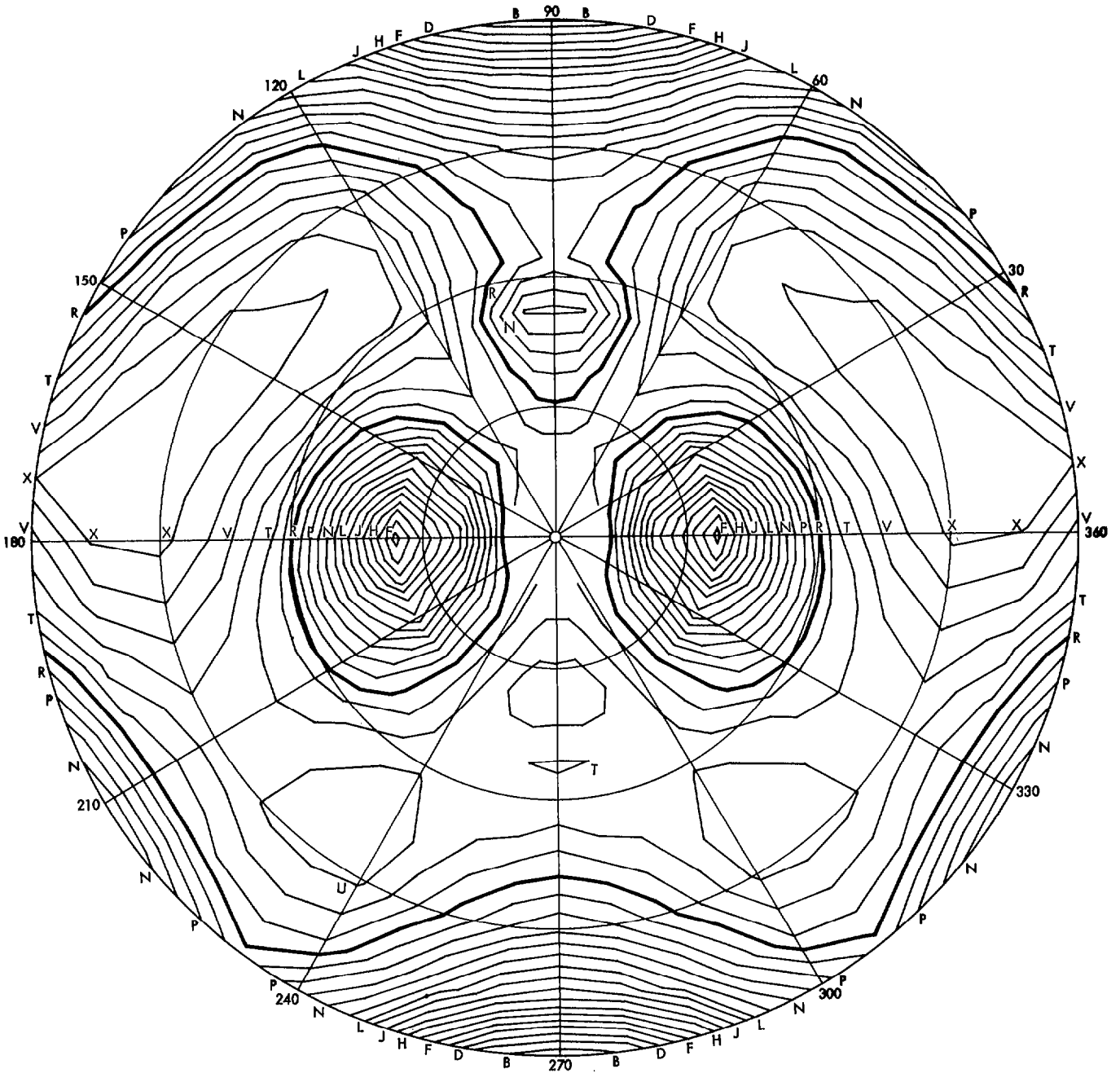

CONTOUR DEFINITIONS

NORMAL ERROR, mm	LABEL	NORMAL ERROR, mm	LABEL	NORMAL ERROR, mm	LABEL
-2.55	A	-1.20	J	0.15	S
-2.40	B	-1.05	K	0.30	T
-2.25	C	-0.90	L	0.45	U
-2.10	D	-0.75	M	0.60	V
-1.95	E	-0.60	N	0.75	W
-1.80	F	-0.45	O	0.90	X
-1.65	G	-0.30	P	1.05	Y
-1.50	H	-0.15	Q	1.20	Z
-1.35	I	0.00	R		

Fig. 5. Horizon-look (panels set at 45-deg elevation) normal errors to best-fit paraboloid for existing 64-m antenna; rms = 0.63 mm (0.025 in.)

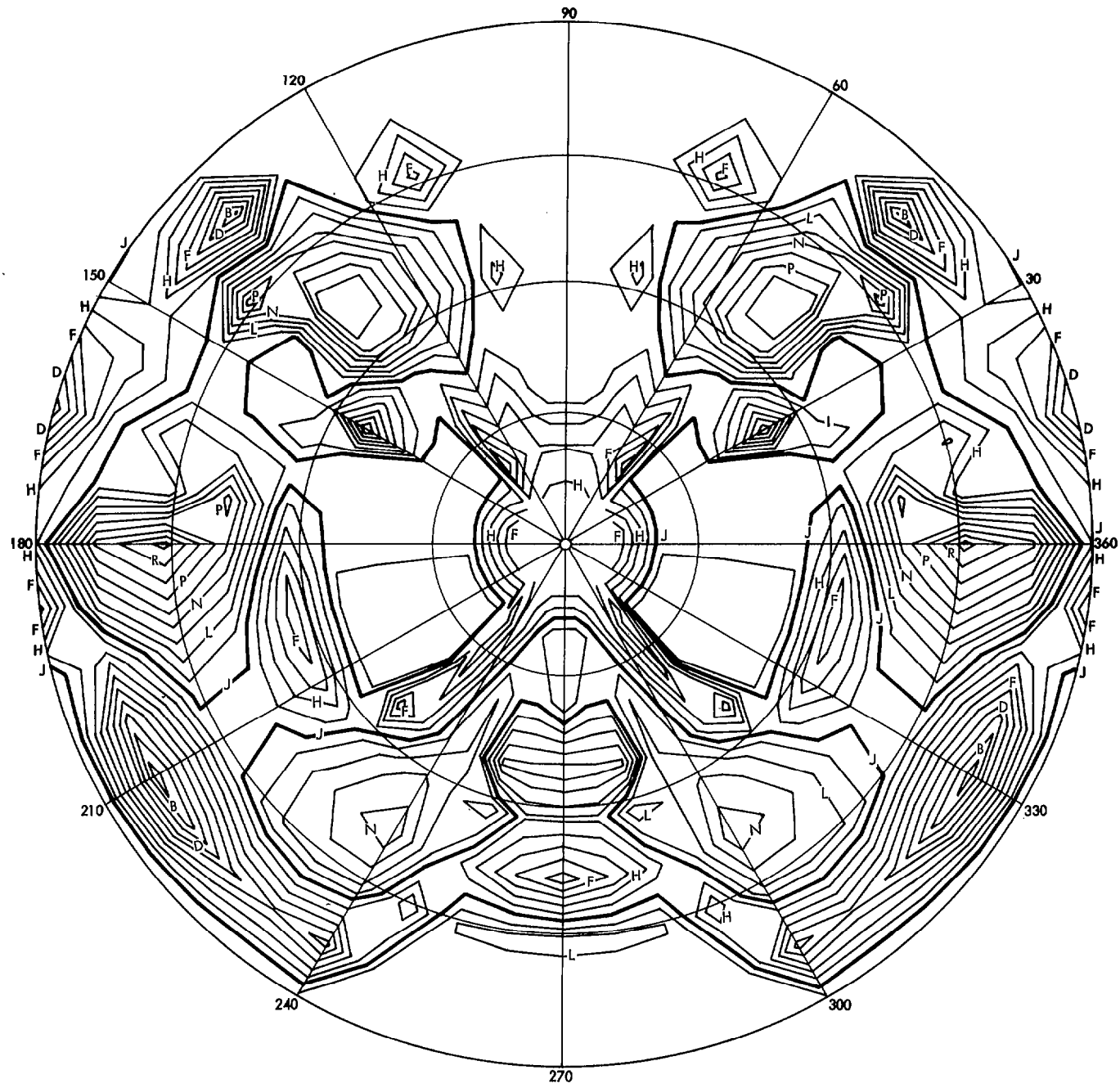

CONTOUR DEFINITIONS

NORMAL ERROR, mm	LABEL	NORMAL ERROR, mm	LABEL	NORMAL ERROR, mm	LABEL
-0.45	A	-0.10	H	0.25	O
-0.40	B	-0.05	I	0.30	P
-0.35	C	0.00	J	0.35	Q
-0.30	D	0.05	K	0.40	R
-0.25	E	0.10	L	0.45	S
-0.20	F	0.15	M		
-0.15	G	0.20	N		

Fig. 6. Horizon-look (panels set at 45-deg elevation) normal errors to best-fit paraboloid with option-1 corrections; rms = 0.15 mm (0.006 in.)

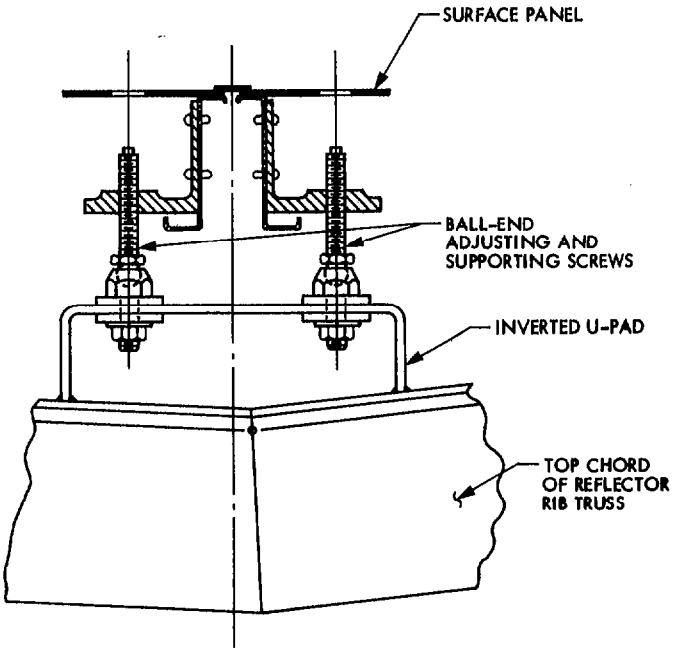

Fig. 7. Typical surface panel support

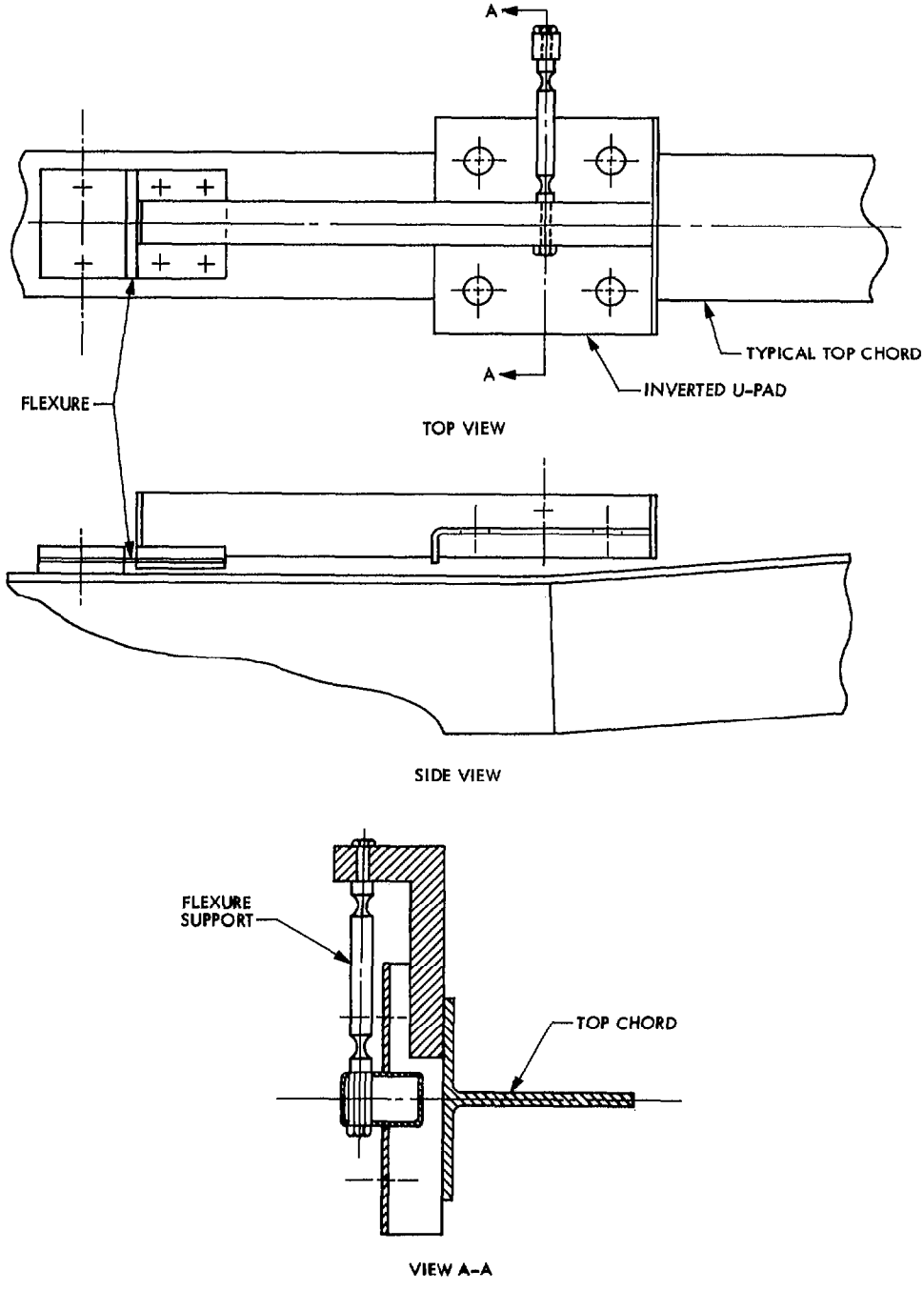

Fig. 8. Proposed pivoted inverted U-pad

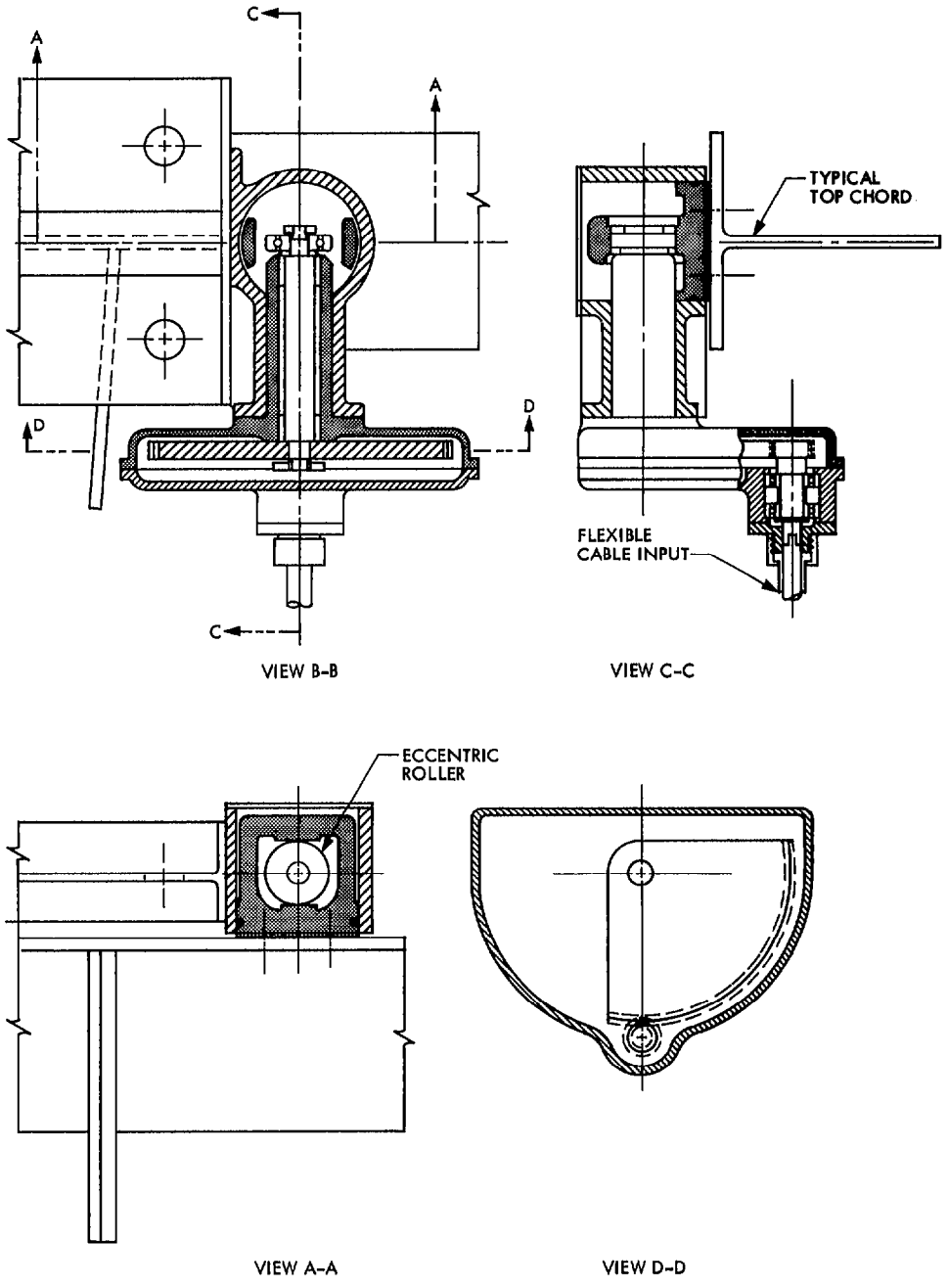

Fig. 9. Proposed eccentric roller assembly